

# Supporting Information

## A Strategy for the Synthesis of Cyclomatrix-polyphosphazene

### Nanoparticles from Non-aromatic Monomers

Zhangjun Huang<sup>a</sup>, Feng Zheng<sup>a</sup>, Shuangshuang Chen<sup>a</sup>, Xuemin Lu<sup>a</sup>, Cornelia Gertina Catharina  
Elizabeth van Sittert<sup>b</sup> and Qinghua Lu<sup>a\*</sup>.

<sup>a</sup> School of Chemistry and Chemical Engineering, the State Key Laboratory of Metal Matrix  
Composites, Shanghai Jiaotong University, Shanghai, P. R. China;

<sup>b</sup> Catalysis and Synthesis Research Group, Chemical Resource Beneficiation Focus Area, North-  
West University, Potchefstroom, South Africa

## Outline

- S1.  $^1\text{H}$ ,  $^{13}\text{C}$  and  $^{31}\text{P}$  NMR study of the oligomers (under the molar feed ratio of 1:3)
- S2. GPC analysis of the PPZ-CysM, PPZ-LysM and PPZ-ArgM oligomer solutions
- S3. MS analysis of the PPZ-CysM, PPZ-LysM and PPZ-ArgM oligomers
- S4. SEM analysis of C-PPZ precipitates morphologies when  $\delta_m$  is lower than UCSP
- S5. SEM analysis of C-PPZ precipitates morphologies when  $\delta_m$  exceeds LCSP
- S6. DSC and TGA analysis of PPZ-CysM nanoparticles
- S7. Solid-state  $^{31}\text{P}$  NMR and EDS analysis of PPZ-CysM nanoparticles
- S8. IR analysis of PPZ-CysM nanoparticles prepared under different molar feed ratios
- S9. DLS analysis and yield of C-PPZ nanoparticles prepared at different molar feed ratios
- S10. Weight-measuring method for nanoparticles yield calculations
- S11. Computational Theory
- S12. Computational method and model establishment
- S13. Sample calculation for  $\chi$
- S14. References for SI

S1.  $^1\text{H}$ ,  $^{13}\text{C}$  and  $^{31}\text{P}$  NMR study of the oligomers (under the molar feed ratio of 1:3)

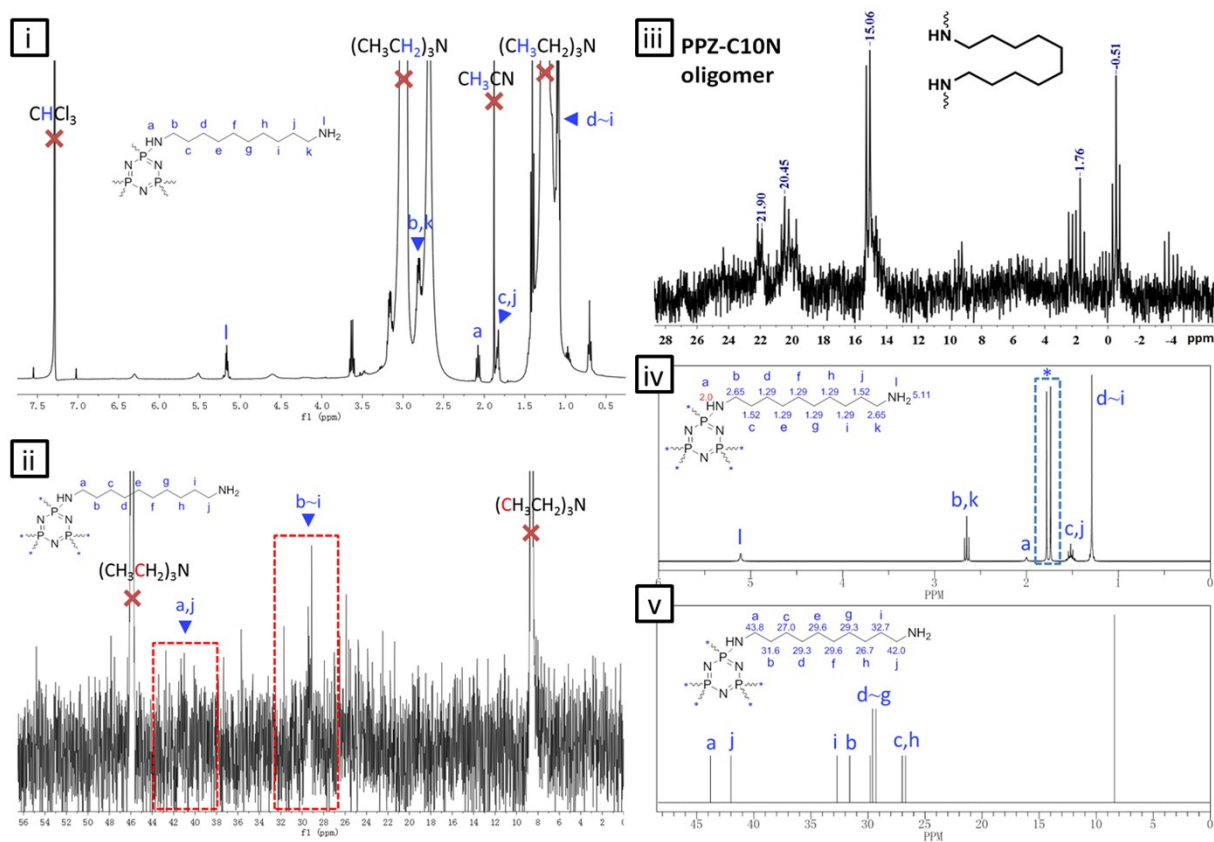


Figure S1a. i)  $^1\text{H}$ , ii)  $^{13}\text{C}$  and iii)  $^{31}\text{P}$  NMR of PPZ-C10N oligomer. The corresponding computer simulation of iv)  $^1\text{H}$  and v)  $^{13}\text{C}$  NMR of PPZ-C10N oligomer.

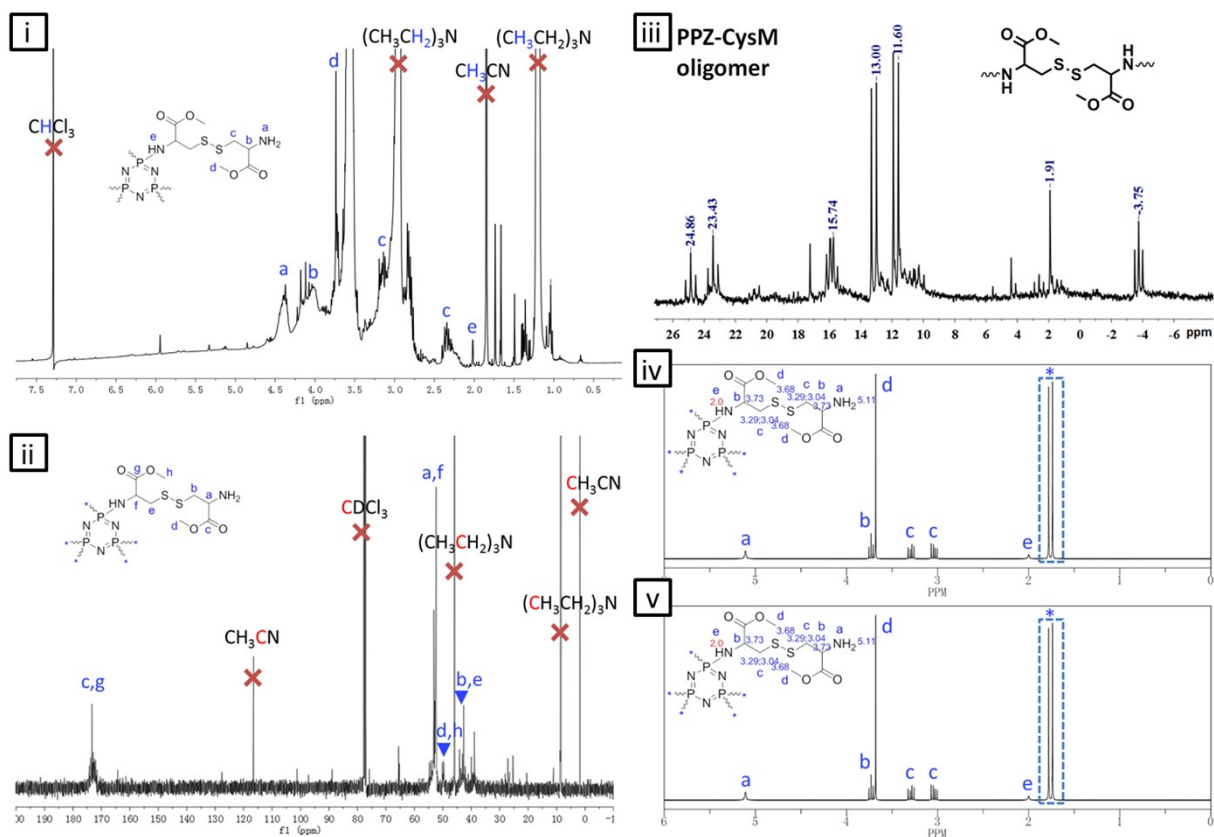


Figure S1b. i)  $^1\text{H}$ , ii)  $^{13}\text{C}$  and iii)  $^{31}\text{P}$  NMR of PPZ-CysM oligomer. The corresponding computer simulation of iv)  $^1\text{H}$  and v)  $^{13}\text{C}$  NMR of PPZ-CysM oligomer.

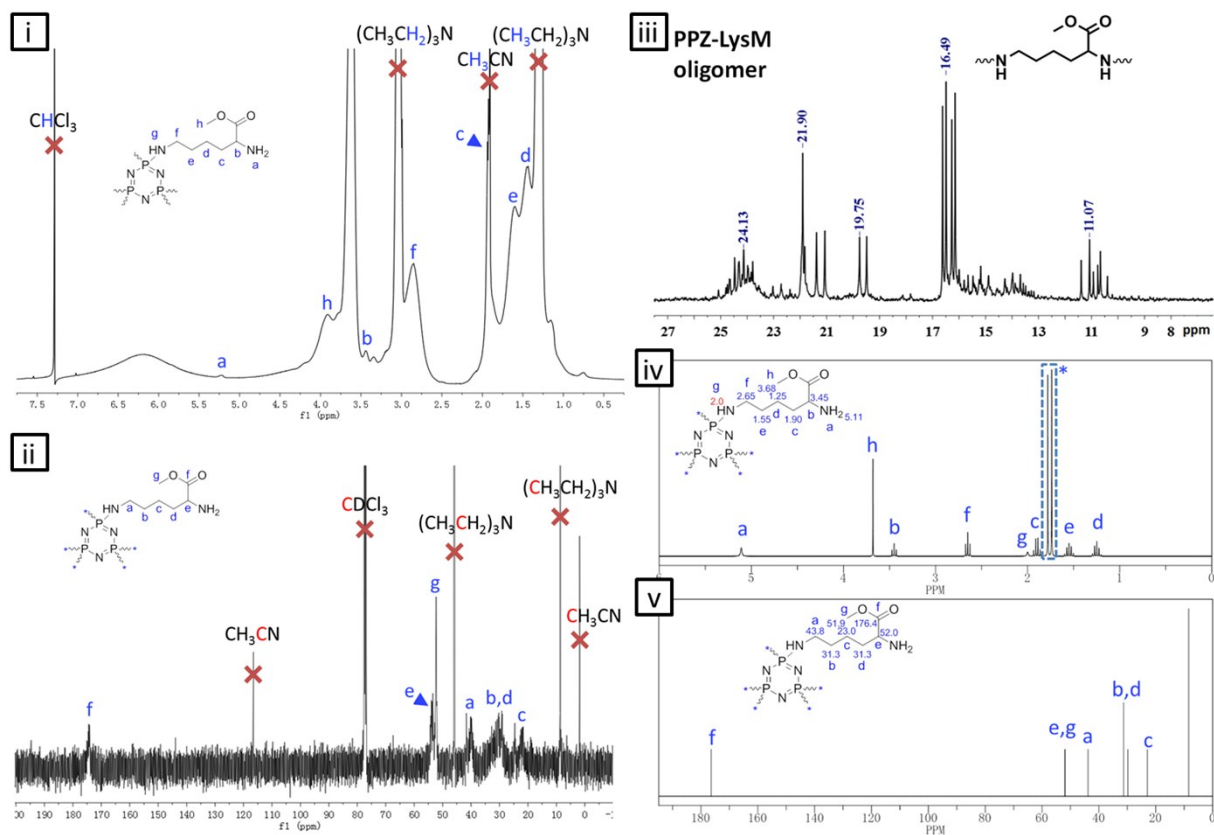


Figure S1c. i)  $^1\text{H}$ , ii)  $^{13}\text{C}$  and iii)  $^{31}\text{P}$  NMR of PPZ-LysM oligomer. The corresponding computer simulation of iv)  $^1\text{H}$  and v)  $^{13}\text{C}$  NMR of PPZ-LysM oligomer.

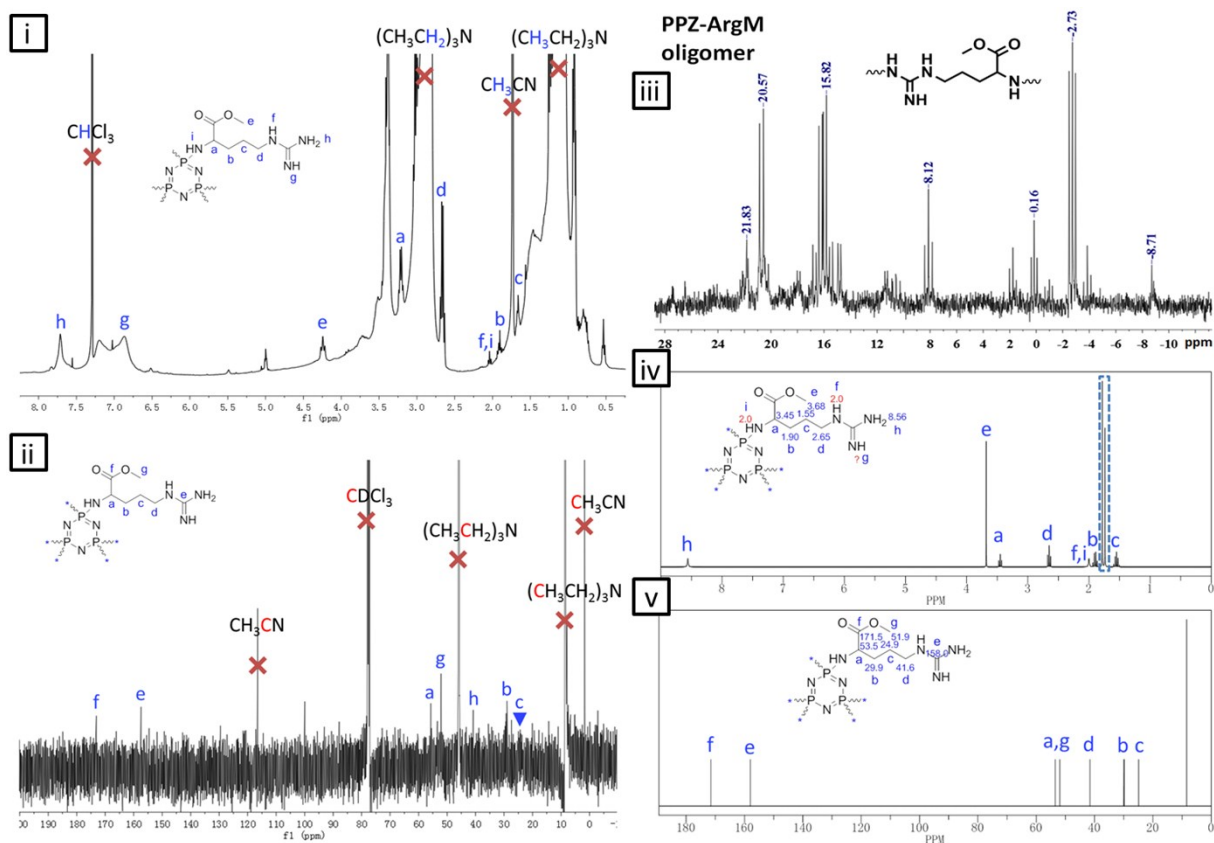


Figure S1d. i)  $^1\text{H}$ , ii)  $^{13}\text{C}$  and iii)  $^{31}\text{P}$  NMR of PPZ-ArgM oligomer. The corresponding computer simulation of iv)  $^1\text{H}$  and v)  $^{13}\text{C}$  NMR of PPZ-ArgM oligomer.

## S2. GPC analysis of the PPZ-CysM, PPZ-LysM and PPZ-ArgM oligomer solutions

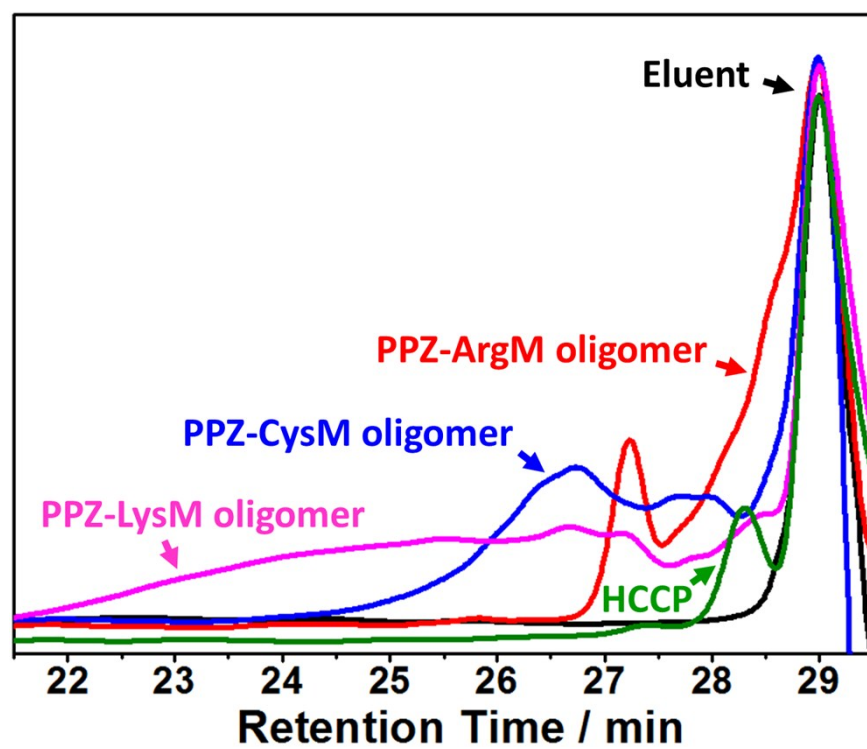


Figure S2. GPC analysis of eluent (DMF, black), HCCP (green), PPZ-CysM oligomer (blue), PPZ-LysM oligomer (violet) and PPZ-ArgM oligomer (red).

### S3. MS analysis of the PPZ-CysM, PPZ-LysM and PPZ-ArgM oligomers

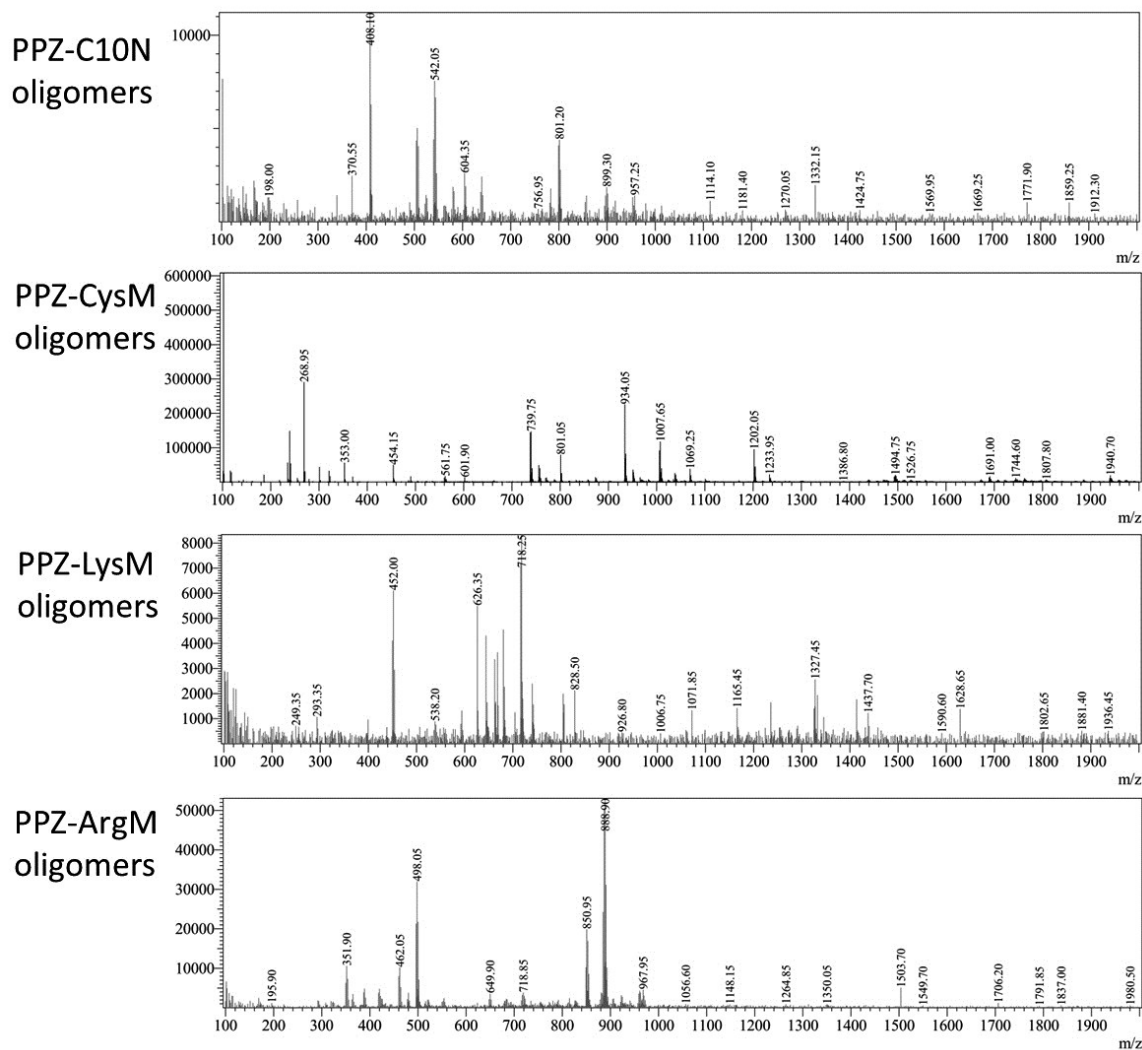


Figure S3. MS analysis of PPZ-C10N oligomers, PPZ-CysM oligomers, PPZ-LysM oligomers and PPZ-ArgM oligomers, respectively.



**S4. SEM study of the C-PPZ precipitates morphologies when  $\delta_m$  is lower than UCSP**

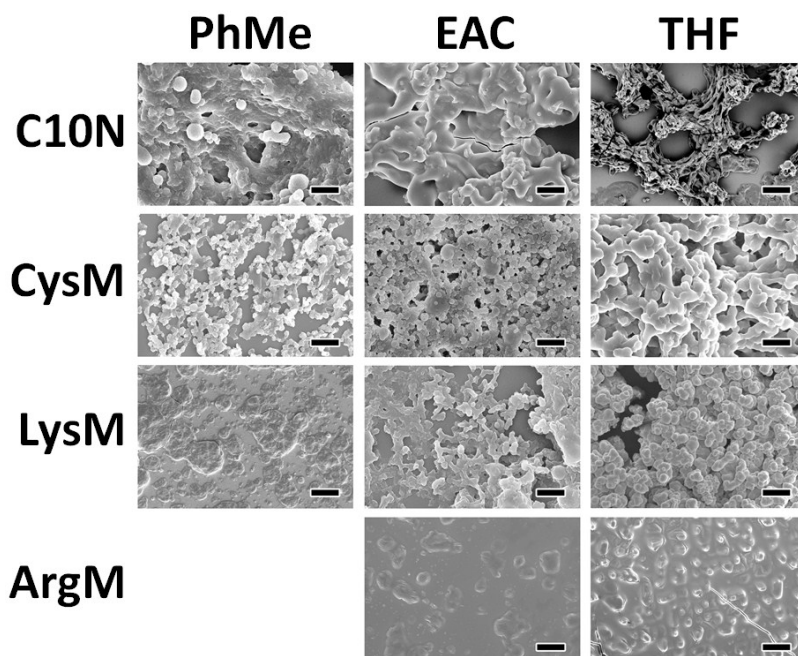


Figure S4. SEM morphology matrix of C-PPZ precipitates prepared when  $\delta_m$  is lower than UCSP. The longitudinal variable is the organic monomers, and the lateral variable is the organic solvents for C-PPZ oligomers. Abbreviations of PhMe and EAC refer to toluene and ethyl acetate, respectively. Scale bar is 2  $\mu\text{m}$ .

**S5. SEM study of the C-PPZ precipitates morphologies when  $\delta_m$  surpasses LCSP**

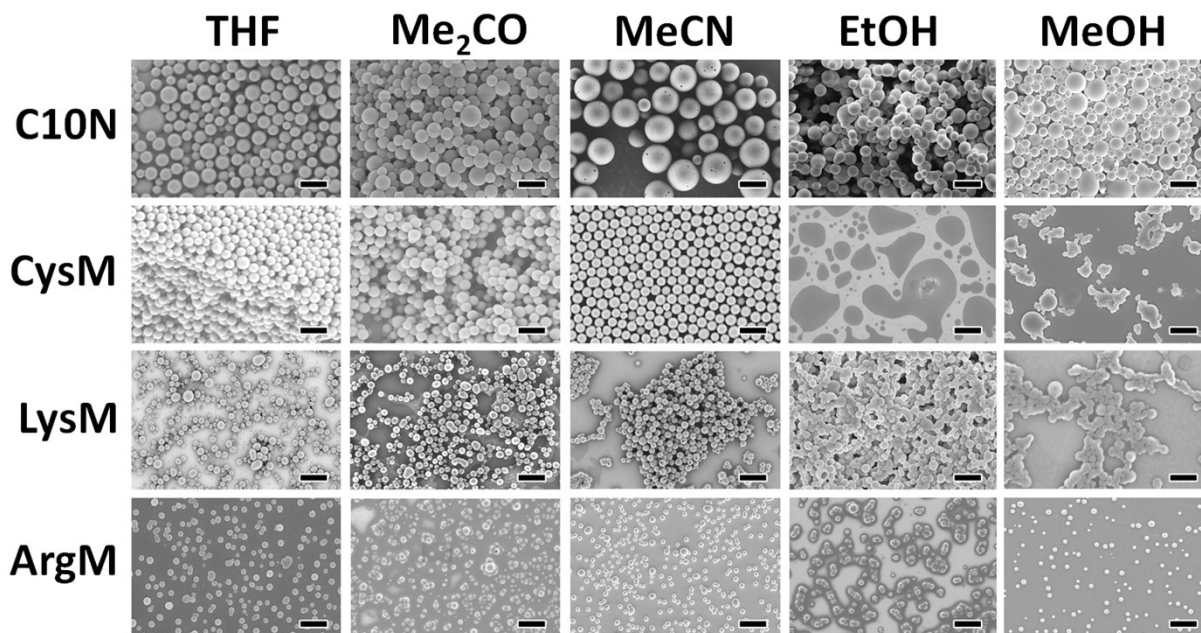


Figure S5. The SEM morphologies matrix of C-PPZ precipitates prepared when  $\delta_m$  exceeds LCSP. The longitudinal variable is the organic monomers, and the lateral variable is the organic solvents for the C-PPZ oligomers. Abbreviations of C10N, CysM, LysM and ArgM refer to PPZ-C10N, PPZ-CysM, PPZ-LysM, PPZ-ArgM, respectively. THF, Me<sub>2</sub>CO, MeCN, EtOH and MeOH are solvents tetrahydrofuran, acetone, acetonitrile, ethanol, and methanol, respectively. Scale bar is 2 μm.

## S6. DSC and TGA analysis of PPZ-CysM nanoparticles

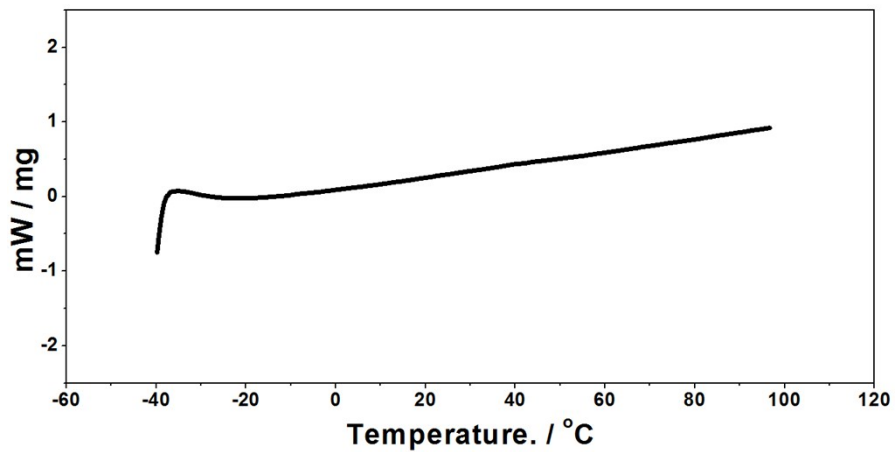


Figure S6a. DSC curve of PPZ-CysM particles.

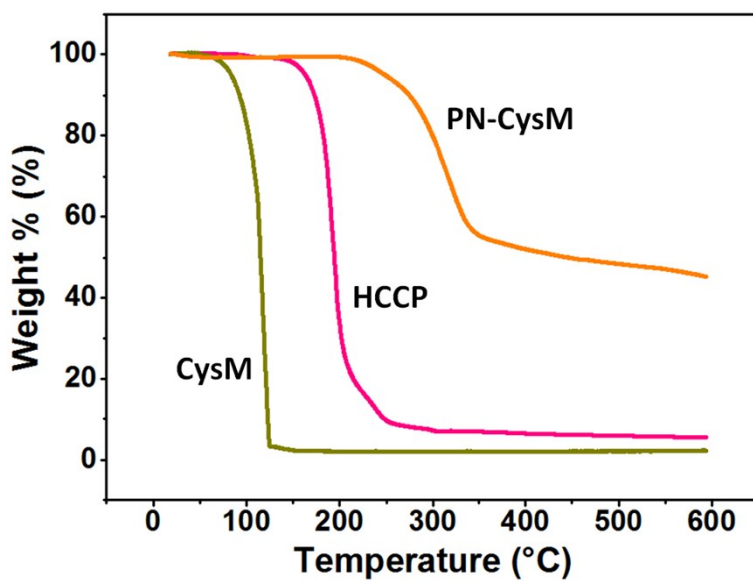


Figure S6b. TGA curve of cystine methyl ester, HCCP and PPZ-CysM particles.

## S7. Solid-state $^{31}\text{P}$ NMR and EDS analysis of PPZ-CysM nanoparticles

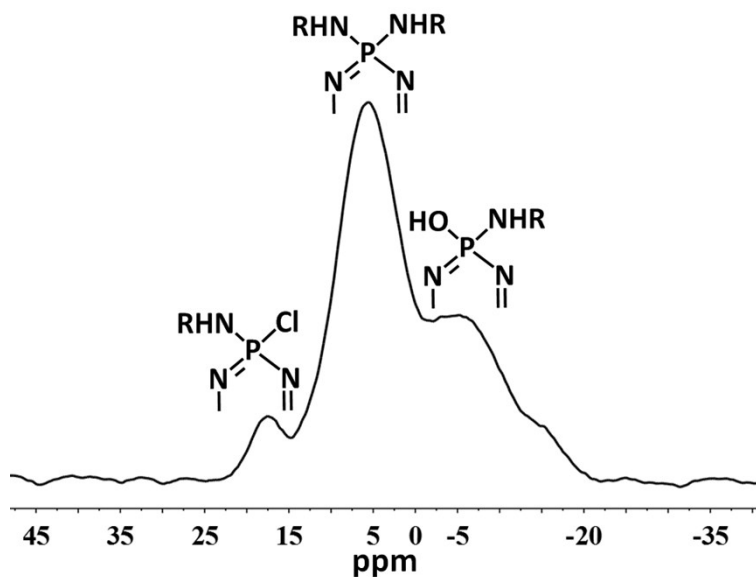


Figure S7a. The solid-state  $^{31}\text{P}$  NMR of PN-CysM particles. Chemical shifts are referred to external  $\text{KH}_2\text{PO}_4$  (0 ppm).

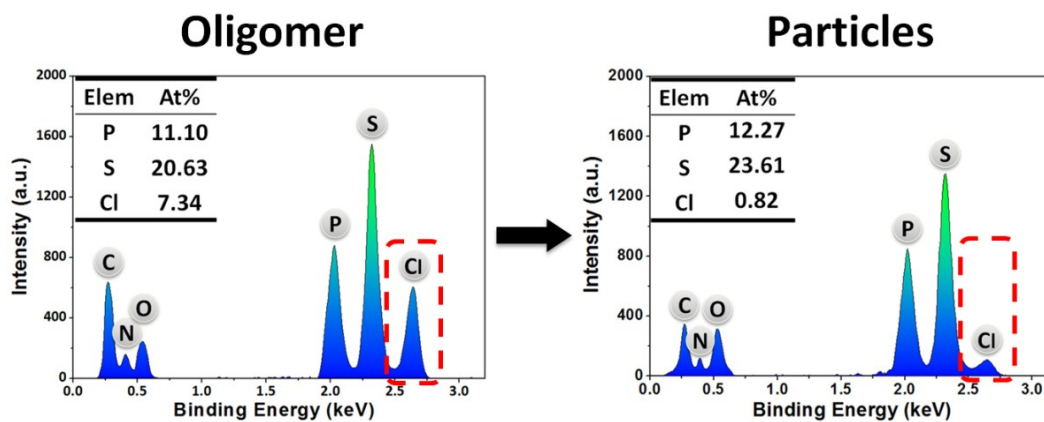


Figure S7b. The comparison of EDS data of PPZ-CysM oligomer and particles.

## S8. IR analysis of PPZ-CysM nanoparticles prepared under different molar feed ratios

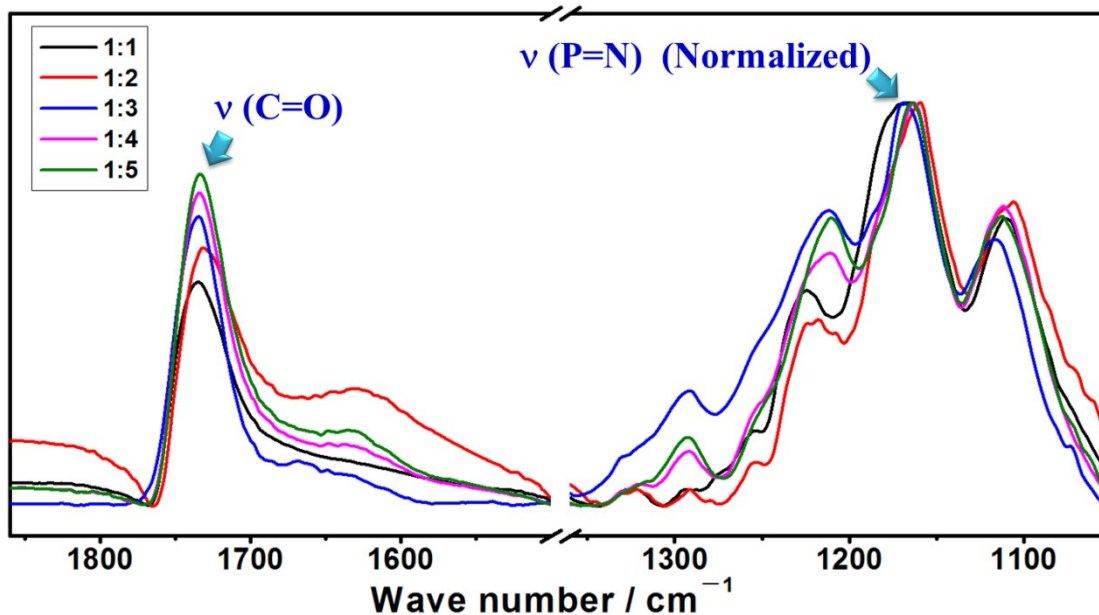


Figure S8a. IR analysis of PPZ-CysM nanoparticles prepared under different molar feed ratios from 1:1 to 1:5. The peak at  $1735\text{ cm}^{-1}$  refers to the C=O stretch vibration of CysM, whereas that at  $1166\text{ cm}^{-1}$  refers to the P=N stretch vibration of the cyclophosphazene ring. The IR absorption intensity has been normalized. After normalization of the IR absorption intensity of the  $\nu(\text{P}=\text{N})$  peaks, linear fitting result of the IR absorption intensity of  $\nu(\text{C}=\text{O})$  is presented in Fig. S8b.

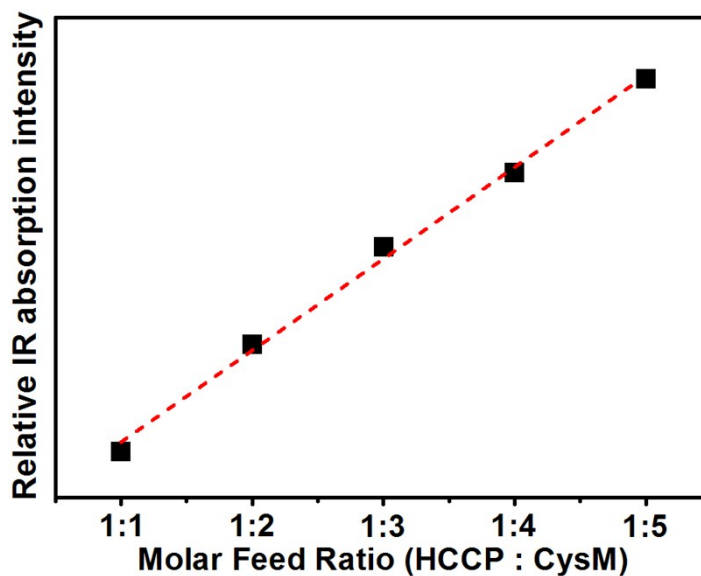


Figure S8b. Linear fitting of IR absorption intensity at  $1735\text{ cm}^{-1}$ .

S9. DLS analysis and yield of C-PPZ nanoparticles prepared at different molar feed ratios.

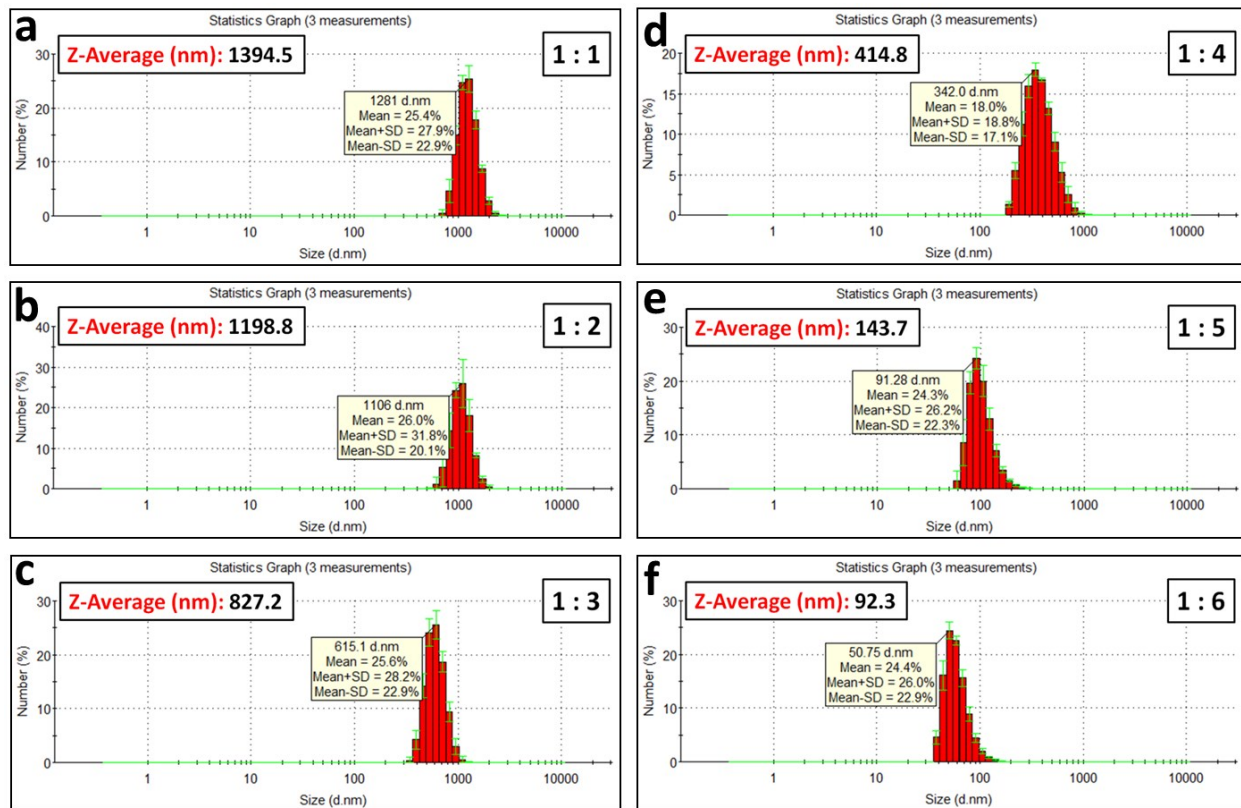


Figure S9a. DLS analysis of PPZ-CysM nanoparticles prepared at molar feed ratios from 1:1 to 1:6.

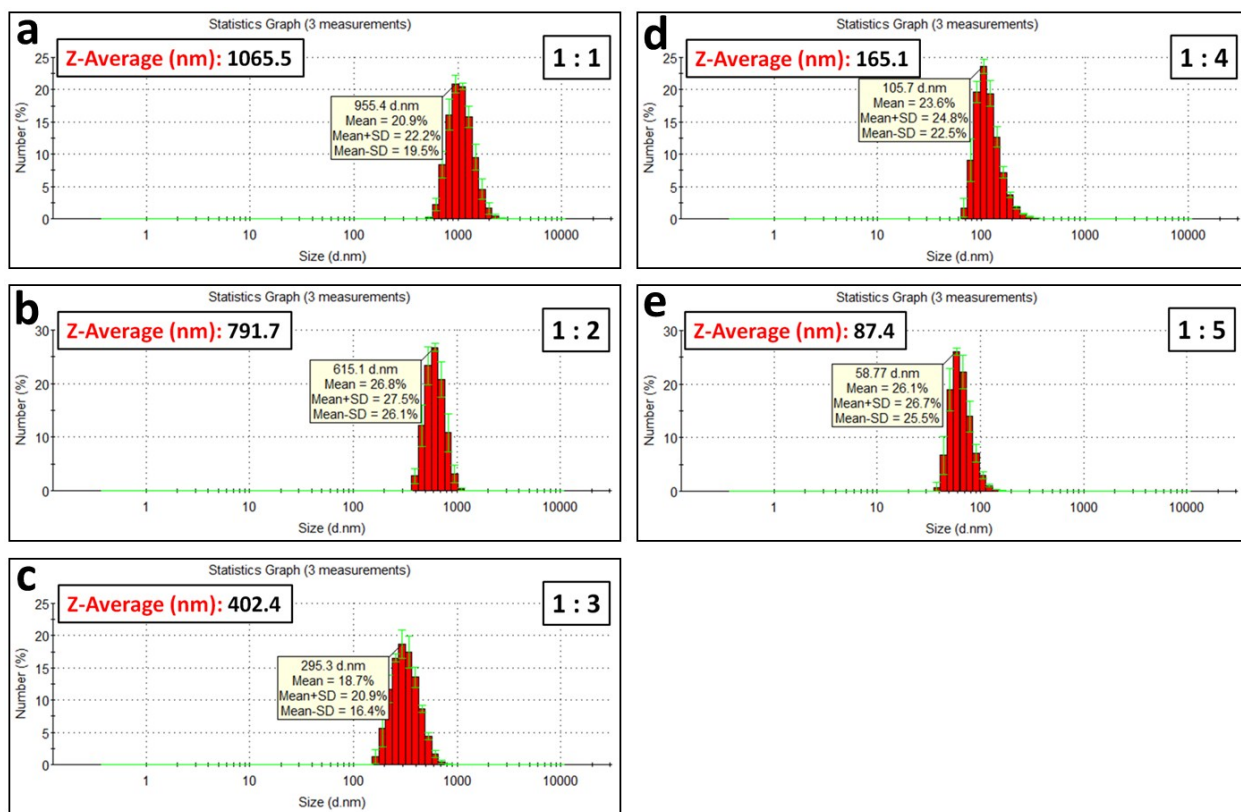


Figure S9b. DLS analysis of PPZ-LysM nanoparticles prepared at molar feed ratios from 1:1 to 1:5.

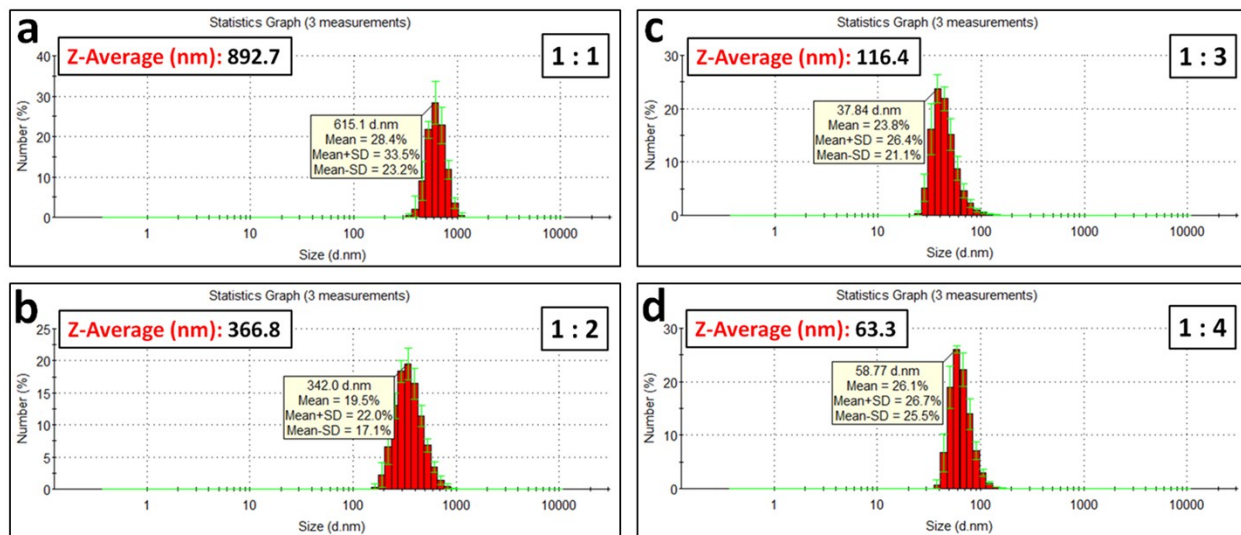


Figure S9c. DLS analysis of PPZ-ArgM nanoparticles prepared at molar mole ratios from 1:1 to 1:4.

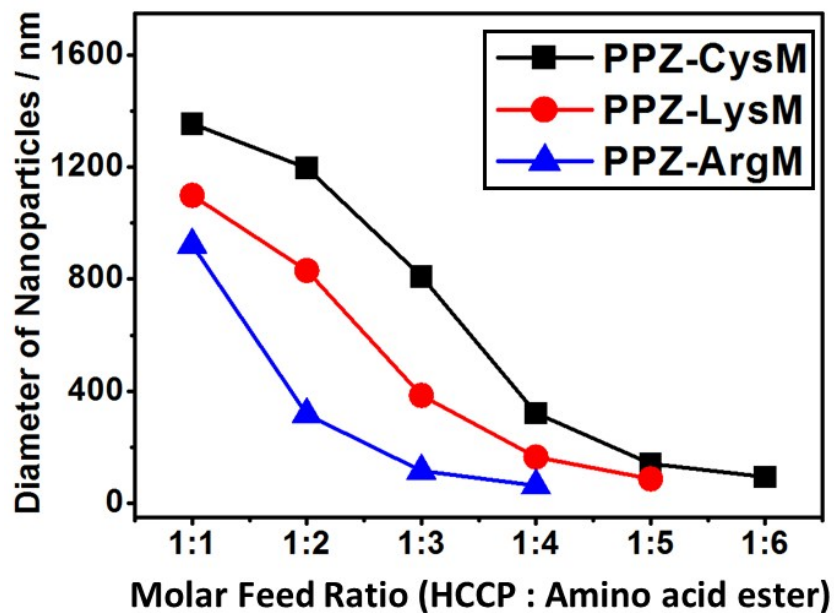


Figure S9d. Change in nanoparticle diameter of PPZ-CysM, PPZ-LysM and PPZ-ArgM nanoparticles with increase in molar feed ratio of HCCP to corresponding amino acid esters.

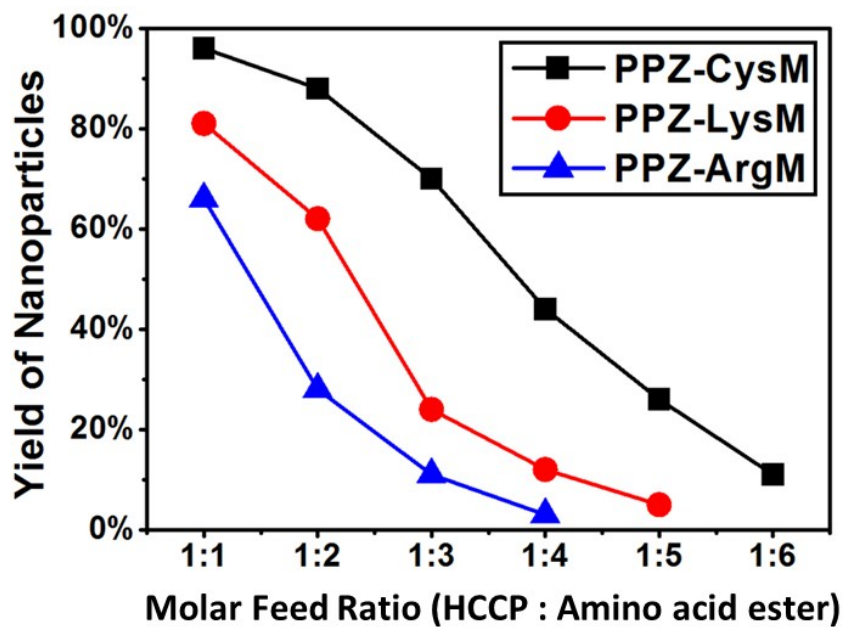


Figure S9e. Change in nanoparticle yield of PPZ-CysM, PPZ-LysM and PPZ-ArgM nanoparticles with increase in molar feed ratio of HCCP to corresponding amino acid esters.



### S10. Weight-measuring method for nanoparticles yield calculations.

Table S1. List of actual mass, theoretical mass and yield for each C-PPZ nanoparticle products.

Sample name	Molar feed ratio	Actual mass (g)	Theoretical mass (g)	Yield
PPZ-CysM	1:1	1.677	1.747	96%
	1:2	2.195	2.494	88%
	1:3	2.269	3.241	70%
	1:4	1.754	3.986	44%
	1:5	1.231	4.733	26%
	1:6	0.603	5.480	11%
PPZ-LysM	1:1	1.096	1.353	81%
	1:2	1.060	1.710	62%
	1:3	0.496	2.066	24%
	1:4	0.291	2.422	12%
	1:5	0.139	2.776	5%
	1:6	--	3.132	--
PPZ-ArgM	1:1	0.946	1.434	66%
	1:2	0.524	1.871	28%
	1:3	0.254	2.307	11%
	1:4	0.082	2.744	3%
	1:5	--	3.178	--
	1:6	--	3.615	--

Note: Actual mass =  $m_{(\text{sample}+\text{tube})} - m_{\text{tube}}$

## Computational Part:

### S11. Computational Theory

A simple definition for a “solubility parameter  $\delta$ ” was proposed by Hildebrand in 1936 and provides a systemic description of the miscibility behavior of solvents. For a pure liquid substance, it is defined as the square root of the cohesive energy density, which is the heat of vaporization divided by the molar volume.

$$\delta = \sqrt{\frac{(\Delta H_v - RT)}{V_m}} \quad (S1)$$

where  $\Delta H_v$  is the heat of vaporization, and  $V_m$  is the molar volume.  $RT$  is the ideal gas  $pV$  term, and it is subtracted from the heat of vaporization to obtain an energy of vaporization.

Hansen then proposed an extension of the Hildebrand parameter method, which is termed the “3D solubility parameter”, to estimate the relative miscibility of polar and hydrogen-bonding systems. In this approach the Hildebrand solubility parameter is split into three components: polar, dispersion and hydrogen bonding.

$$\delta^2 = \delta_d^2 + \delta_p^2 + \delta_h^2 \quad (S2)$$

These two quantities represented by Eqs (S1) and (S2) are expected to be similar but not identical. For polymers, the Hansen parameters are assigned to the solubility parameters, which causes the maximum swelling in a series of polymer swelling experiments. Besides this, a variety of other experimental methods are also used, which leads to a wide range of experimentally reported values.<sup>1</sup>

From the Hildebrand and Hansen solubility parameter, one can determine the polymer–solvent miscibility through the Flory–Huggins (FH) theory.<sup>2</sup> The theory describes the solvent–solute interaction through an effective parameter termed the Flory–Huggins interaction parameter  $\chi$ . There are two approaches have been reported in the literature to calculate  $\chi$  by atomistic simulations: (i) an approximate one based on the Hildebrand and Hansen solubility parameters of the isolated components,<sup>3</sup> and (ii) a more accurate one based on an evaluation of the enthalpy of mixing by simulating also the mixed phase.

The first approach has been followed by different authors according to:<sup>4</sup>

$$\chi = \frac{V(\delta_S - \delta_P)^2}{RT} \quad (\text{S3})$$

where  $V$  is the molar volume of the solvent and  $RT$  has the usual meaning. This method completely neglects the specific interactions between solute and solvent as no simulation of the mixed phase was required, and positive values of  $\chi$  are always given, although the negative values are common in a real system.

A more accurate method was also reported in literature with applications on evaluating the miscibility binary system, such as a drug–polymer,<sup>5</sup> and a polymer–solvent system,<sup>6</sup> by means of molecular dynamics (MD). Solution behavior is governed by the Gibbs free energy change that accompanies mixing,  $\Delta G_m$ . If  $\Delta G_m$  is negative, two or more substances are miscible, otherwise they are immiscible.  $\Delta G_m$  can be calculated according to Eq (S4) based on the Flory–Huggins solution theory for polymers<sup>2</sup>.

$$\Delta G_m = KT[n_S \ln(\phi_S) + n_P \ln(\phi_P) + n_S \chi_{FH} \phi_P] \quad (\text{S4})$$

where  $n_s$  and  $n_p$  are the number of molecules and  $\Phi_s$  and  $\Phi_p$  are the volume fractions of the solvent(s) and polymer (p), respectively.

The Flory–Huggins interaction parameter  $\chi$  is a dimensionless parameter that describes the polymer–solvent interaction strength and it controls the solubility. The  $\chi_{FH}$  value at room temperature can be obtained according to the equation

$$\chi = \frac{V_{ref} \Delta H_m}{kT V_m \Phi_s \Phi_p} \quad (S5)$$

where  $V_{ref}$  is the reference volume, which is taken equal to the volume of the smallest molecule in the solution and  $\Delta H_m/V_m$  is the change in enthalpy upon mixing per unit volume. The later can be calculated by MD from the cohesive energy densities of pure solvent,<sup>7,8</sup> pure polymer and solvent-polymer mixture,<sup>9</sup> by Eq. (S6).

$$\frac{\Delta H_m}{V_m} = CED_m - (CED_s \Phi_s + CED_p \Phi_p) \quad (S6)$$

The CED of a system describes the energy required to remove an atom from the molecule, and it is related to the heat of vaporization  $\Delta H_v$ , by Eq (S7).

$$CED = \frac{\rho}{M} (\Delta H_v - RT) \quad (S7)$$

The CED was calculated by the Forcite module of Materials Studio. In this module, the total energy,  $E_{tot}$ , is calculated for an isolated molecule and for the bulk system with periodic boundary conditions using Eq. (S8).

$$E_{tot} = E_{bonded} + E_{nonbonded} \quad (S8)$$

The heat of vaporization is related to these values as described in Eq (S9), and the solubility parameter  $\delta$ , is calculated from CED according to Eq. (S10).

$$\Delta H_v = \langle E_{tot,bulk} - E_{tot,molecules} \rangle + RT \quad (S9)$$

$$\delta = \sqrt{CED} \quad (S10)$$

It has been shown that molecular dynamics simulation with the isothermal-isobaric ensemble (NPT-MD simulation) is accurate in predicating many solubility parameters of both solvents and polymers.<sup>10</sup>

## **S12. Computational method and model establishment**

MD simulations with the COMPASS (Condensed-phase Optimized Molecular Potentials for Atomistic Simulation Studies) force field of pure solvents, pure PPZ-CysM oligomers and oligomer–solvent systems were presented. A multi-sample MD method reported previously by Belmares et al. was used in this study.<sup>10</sup> This method is particularly useful in rapidly generating polymer structures with large monomer units containing rings or other complex groups.

### **PPZ-CysM model.**

Experimentally, crystal structures of similar compounds were reported where Cl-substitution favors chlorine atoms attached to the same phosphorous atom.<sup>11,12</sup> The PPZ-CysM oligomers were found to be composed of substituted monomers and dimers (see Fig. S10) with 33% of unreacted chlorine on the HCCP ring in our work.<sup>13</sup> Theoretically, the charge of all chlorine atoms and the relative strength of all P-Cl bonds in one substituted HCCP structure was compared on a molecular level. It has been proven from the electronic charge (Fig. S11a) or from the bond strength, which related to the bond length (Fig. S11b), that the chlorine atom on

the substituted cyclotriphosphazene is the most favored one for nucleophilic attack. Therefore, the model PPZ-CysM oligomer that was built as shown in Fig. S11c.

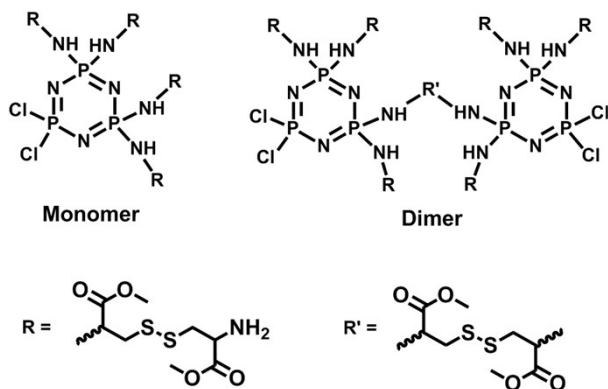


Figure S10. Model structures for PPZ-CysM oligomers for MD simulation.

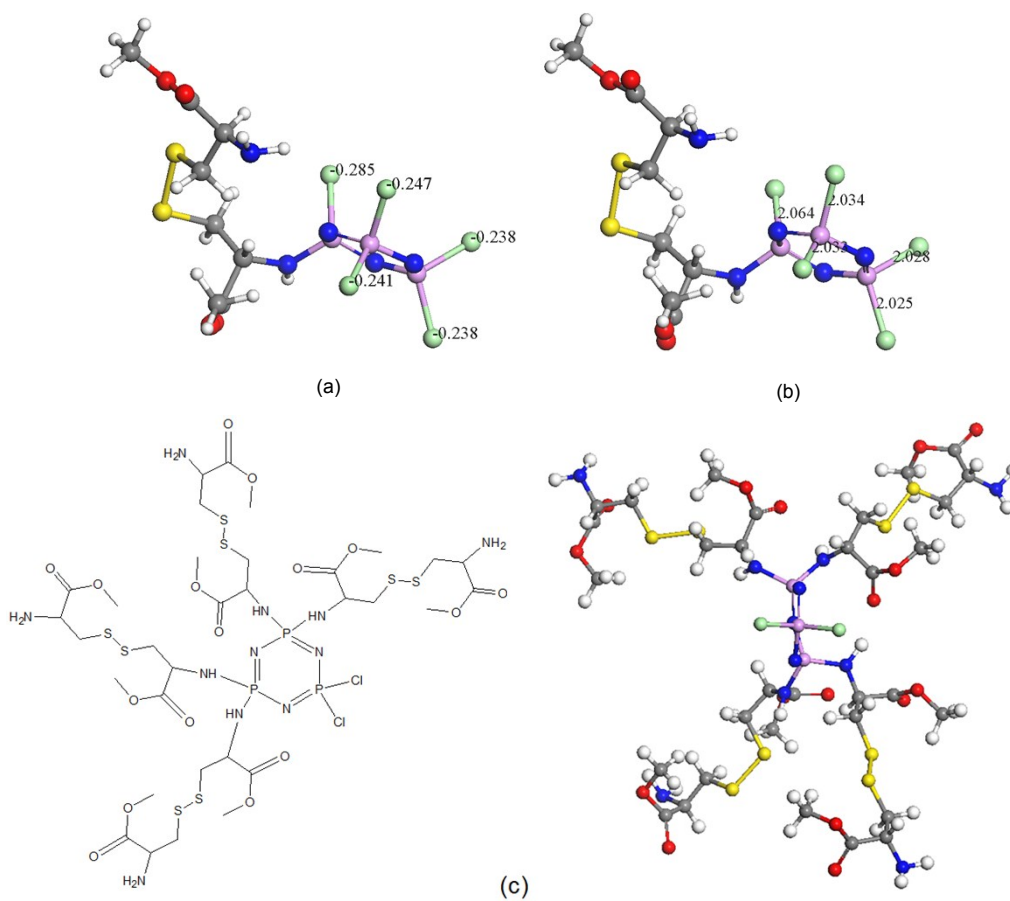


Figure S11. Optimized structure of one CysM substituted HCCP with (a) electronic charge, (b) bond length, (c) the model PPZ-CysM oligomer for MD simulation.

## **Amorphous cell**

A periodic cell for each system (pure solvent, pure oligomers, and oligomer-solvent mixture) was created using the Amorphous Cell module in Materials Studio following the method reported by Belmares et al.<sup>10</sup> During cell construction, the density was ramped from 0.4 to 1.5 g/cm<sup>3</sup> at 500 K. The periodic cell minimization was compared with the Discover and Forcite modules. Cyclohexane was used as a model solvent to validate the cell optimization method. As shown in Table S2, the cell was minimized using the Geometry Optimization model of Forcite and utilizing the steepest descent method, followed by the conjugated method, and finally the Quasi-Newton method (method III) was found to be most accurate result compared with the experimental values.

The Forcite module was used in MD calculations. The condensed-phase ab-initio force field, COMPASS was used for all MD calculations. All MD simulations were performed under the isothermal-isobaric ensemble (NPT ensemble). The Anderson thermostat<sup>16</sup> and Berendsen barostat<sup>15</sup> were used to control the temperature and pressure, respectively. The pressure was set to 1 bar (0.00001 Pa) for all simulations. The Ewald summation method was used for van der Waals and columbic interactions was Ewald. Each simulation was run with a time step of 1 fs. The temperature was initially set to 500 K and 50 ps of NPT was performed using the last configuration sampled as a starting configuration. This was followed by 50 ps of NPT dynamics at 400 K, and the final configuration obtained was then used as the starting configuration for NPT dynamics at 298 K. Simulations were run until the average volume and average energy remained constant (no significant drift) for a minimum of 300 ps, which represents system equilibration, as shown in Fig. S12. All data collected represents these final 300 ps of simulation.

Table S2. Comparison of calculated and experimental solubility parameters ( $\delta$ ) and density ( $\rho$ ) for cyclohexane using the NPT\*-MD method. The trend is shown in Fig. S13.

	Sample size	$\delta$ (J/ml) <sup>0.5</sup>	$\rho$ (g/ml)	Method
1		22.479	0.978	I
2	1	20.686	0.913	II
3		17.443	0.808	III
4	5	17.157	0.785	III
5	10	16.805	0.771	III
6	20	16.558	0.794	III
Exp. Value		16.700	0.779	

\* The isothermal-isobaric ensemble (NPT ensemble)

I: Discover/Smart, II: Forcite/Smart, III: Forcite/Three-step method

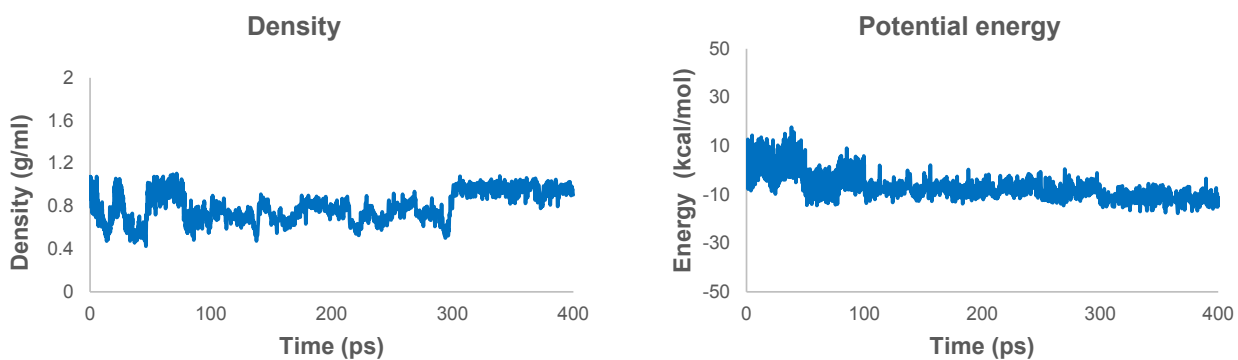


Figure S12. NPT MD statistic on cyclohexane.



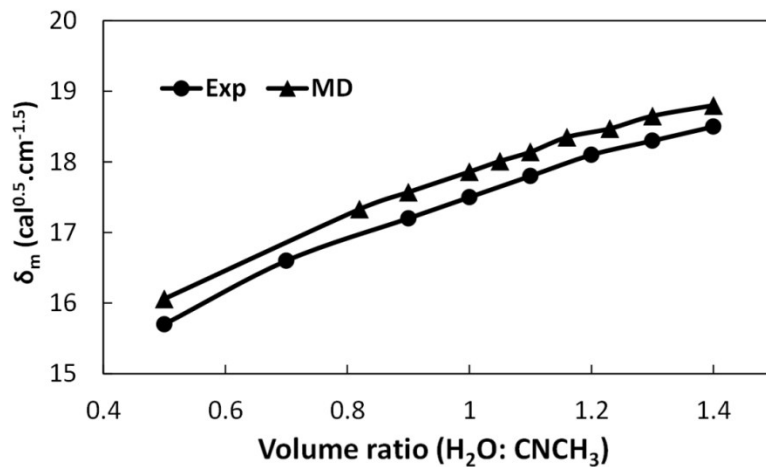


Figure S13. Comparison of computed solubility parameters of mixed solvents with calculated values using Eq (1) for experimental work.

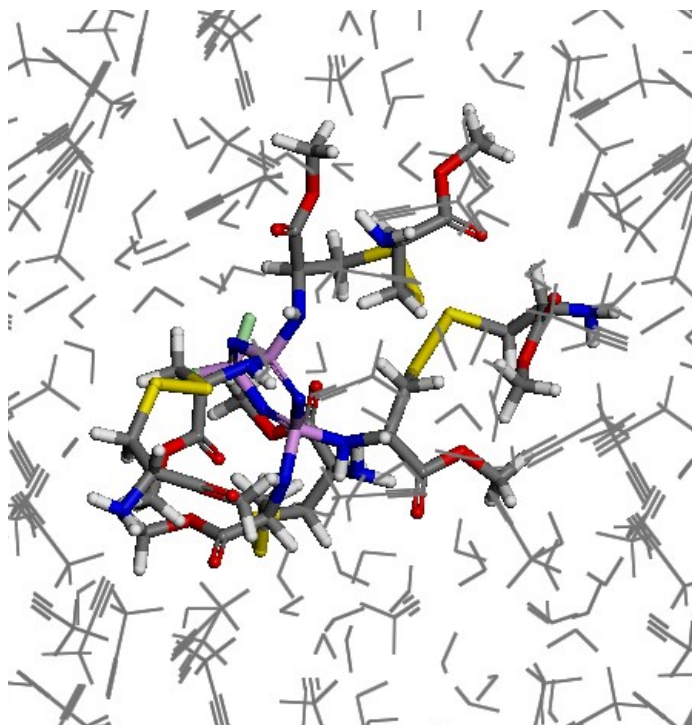


Figure S14. Details of a PPZ-CysM oligomer immersed in H<sub>2</sub>O-MeCN mixed solvent. The solvent molecules are presented in gray, for clarity.

Table S3. Calculated density ( $\rho$ ), CED and solubility parameters ( $\delta$ ) for water–acetonitrile mixed solvents

Solvent	No. of molecules		$\rho$ (g/mL)	CED (J/mL)	$\delta$ (J/ml) <sup>0.5</sup>	$\delta$ (cal/mL) <sup>0.5</sup>
	H <sub>2</sub> O	MeCN				
1	70	30	0.852	1257	35.45	17.34
2	71	29	0.853	1280	35.78	17.49
3	72	28	0.855	1296	36.00	17.60
4	73	27	0.855	1319	36.32	17.76
5	74	26	0.858	1338	36.58	17.89
6	75	25	0.863	1356	36.82	18.01
7	76	24	0.864	1371	37.03	18.11
8	77	23	0.869	1399	37.40	18.29
9	78	22	0.872	1415	37.62	18.39
10	79	21	0.877	1436	37.89	18.53
11	80	20	0.881	1462	38.24	18.70

Table S4. Calculated density ( $\rho$ ), CED, solubility parameters ( $\delta$ ) and interaction parameters ( $\chi$ ) for oligomer–solvent systems (water–acetonitrile mixed solvents)

Oligomer-solvent*	$\rho$ (g/mL)	CED (J/mL)	$\delta$ (J/ml) <sup>0.5</sup>	$\delta$ (cal/ml) <sup>0.5</sup>	$\chi$
1	0.987	1066	32.65	15.97	1.90
2	0.991	1081	32.88	16.08	1.86
3	1.001	1091	33.03	16.15	1.84
4	0.997	1107	33.27	16.27	1.91
5	1.000	1119	33.45	16.36	1.90
6	1.008	1132	33.65	16.45	2.05
7	1.001	1150	33.91	16.58	2.84
8	1.001	1169	34.19	16.72	2.88
9	1.103	1178	34.32	16.78	2.85
10	1.106	1191	34.51	16.88	2.85
11	1.108	1209	34.77	17.00	2.98

\* For oligomer-solvent mixed system, each unit cell contains one PPZ-CysM oligomer and one hundred solvent molecules (solvent composition same as Table S3).

Table S5. Calculated density ( $\rho$ ), CED and solubility parameters ( $\delta$ ) for diethyl ether–acetonitrile mixed solvents

Solvent	No. of molecules		$\rho$ (g/mL)	CED (J/mL)	$\delta$ (J/mL) <sup>0.5</sup>	$\delta$ (cal/mL) <sup>0.5</sup>
	Et <sub>2</sub> O	MeCN				
1	50	50	0.747	364.4	19.09	9.33
2	55	45	0.747	352.5	18.78	9.18
3	56	44	0.745	349.6	18.70	9.14
4	58	42	0.745	344.7	18.57	9.08
5	59	41	0.746	341.0	18.47	9.03
6	60	40	0.744	338.1	18.39	8.99
7	61	39	0.744	336.7	18.35	8.97
8	62	38	0.746	332.6	18.24	8.92
9	64	36	0.740	329.1	18.14	8.87
10	65	35	0.743	325.2	18.03	8.82
11	70	30	0.739	316.0	17.78	8.69

Table S6. Calculated density ( $\rho$ ), CED, solubility parameters ( $\delta$ ) and interaction parameters ( $\chi$ ) for oligomer–solvent systems (diethyl ether–acetonitrile mixed solvents)

Oligomer–solvent*	$\rho$ (g/mL)	CED (J/mL)	$\delta$ (J/ml) <sup>0.5</sup>	$\delta$ (cal/ml) <sup>0.5</sup>	$\chi$
1	0.825	377.8	19.44	9.51	1.90
2	0.819	366.7	19.15	9.36	1.89
3	0.817	364.0	19.08	9.33	1.89
4	0.817	359.4	18.96	9.27	1.87
5	0.815	355.9	18.87	9.23	1.86
6	0.814	354.9	18.84	9.21	2.17
7	0.815	354.9	18.84	9.21	2.42
8	0.814	352.9	18.79	9.18	2.77
9	0.812	351.3	18.74	9.16	3.07
10	0.812	347.2	18.63	9.11	3.01
11	0.811	338.4	18.40	9.00	3.02

\* For oligomer-solvent mixed system, each unit cell contains one PPZ-CysM oligomer and one hundred solvent molecules (solvent composition same as Table S5).

### S13. Sample calculation for $\chi$

The Flory–Huggins interaction parameter  $\chi$  was calculated using Eqs. (S5) and (S6). Here we used the diethyl ether–acetonitrile mixed solvent system (Et<sub>2</sub>O: MeCN = 1: 1) as an example.

$$\frac{\Delta H_m}{V_m} = CED_m - (CED_s \phi_s + CED_p \phi_p) \quad (S6)$$

where,  $CED_m$  and  $CED_s$  are summarized in Tables S4 and S5.  $CED_p$  was reported in the article.

$$\phi_s = \frac{V_s}{V_s + V_p} = \frac{\frac{m_s}{\rho_s}}{\frac{m_s}{\rho_s} + \frac{m_p}{\rho_p}}$$

$$m_s = \frac{\text{no. of molecules} \times \text{molecular weight}}{6.02 \times 10^{23}}$$

$$\phi_s = \frac{\frac{50 \times 41.05}{0.79} + \frac{50 \times 74.12}{0.71}}{\frac{50 \times 41.05}{0.79} + \frac{50 \times 74.12}{0.71} + \frac{1 \times 1275.23}{1.385}} = 0.895$$

$$\phi_p = 1 - \phi_s = 1 - 0.89 = 0.105$$

$$CED_p = 389.2 \text{ J/cm}^3$$

$$\therefore \frac{\Delta H_m}{\Delta V_m} = 377.8 - (364.4 \times 0.89 + 389.2 \times 0.11) = 10. \quad 80$$

$$\chi = \frac{V_{ref} \Delta H_m}{kT V_m \phi_s \phi_p} \quad (S5)$$

where  $V_{ref}$  is the volume of one acetonitrile molecule,  $k = 1.38 \times 10^{23}$

$$\therefore \chi = \frac{6.82 \times 10^{-23}}{1.38 \times 10^{-23} \times 298} \times 10.80 \times \frac{1}{0.895 \times 0.105} = 1.90$$

#### S14. References of SI

- (1) (a) Van Krevelen, D. W. *Properties of Polymers: Their Correlation with Chemical Structure; Their Numerical Estimation and Prediction from Group Contributions*; Elsevier Science Publishers: New York, **1990**, p. 536; (b) Ibid, p. 575.
- (2) Flory, P. J. *J. Chem. Phys.* **1942**, 10, 51.
- (3) Hildebrand, J. H. *Proc. Natl. Acad. Sci. USA* **1979**, 76, 6040.
- (4) (a) Fan, Z. J.; Williams, M. C.; Choi, P. *Polymer* **2002**, 43, 1497; (b) Latere Dwan'Isa, J. P.; Rouxhet, L.; Pr eat, V.; Brewster, M. E.; Ari en, A. *Pharmazie* **2007**, 62, 499; (c) Patel, S.; Lavasanifar, A.; Choi, P. *Biomacromolecules* **2008**, 9, 3014.
- (5) Huynh, L.; Grant, J.; Leroux, J.; Delmas, P.; Allen, C. *Pharm. Res.* **2008**, 25, 147.
- (6) Caddeo, C.; Mattoni, A. *Macromolecules* **2013**, 46, 8003.
- (7) Kasimova, A. O.; Pavan, G. M.; Danani, A.; Mondon, K.; Cristiani, A.; Scapozza, L.; Gurny, R.; M uller, M. *J. Phys. Chem. B* **2012**, 116, 4338.
- (8) Case, F. H.; Honeycutt, J. D. *Trends Polym. Sci.* **1994**, 2, 259.
- (9) Spyriouni, T.; Vergelati, C. *Macromolecules* **2001**, 34, 5306.
- (10) Belmares, M.; Blanco, M.; Goddard, W. A.; Ross, R. B.; Caldwell, G.; Chou, S. H.; Pham, J.; Olofson P. M.; Thomas, C. *J. Comput. Chem.* **2004**, 25, 1814.
- (11) Uslu, A.;  n, S.S.; Kılıç, A.; Yılmaz, S.; Yuksel, F.; Haciveliolu, F. *Inorg. Chim. Acta* **2013**, 405, 140
- (12)  iftçi, G. Y.; Senkuytu, E.; Durmus, M.; Yuksel F.; Kılıç, A. *Inorg. Chim. Acta* **2014**, 423, 489.
- (13) Huang, Z.; Chen, S.; Lu, X.; Lu, Q. *Chem. Commun.* **2015**, 51, 8373.
- (14) Anderson, H. C. *J. Chem. Phys.* **1980**, 72, 2384.
- (15) Berendsen, H. J. C.; Postma, J. P. M.; van Gunsteren, W. F.; DiNola, A.; Haak, J. R. *J. Chem. Phys.* **1984**, 81, 3684.

